Subdivision Depth Computation for Catmull-Clark Subdivision Surfaces

Fuhua (Frank) Cheng
University of Kentucky, Lexington, KY 40506-0046, USA
Jun-Hai Yong
Tsinghua University, Beijing, China

Abstract

A subdivision depth computation technique for Catmull-Clark subdivision surfaces (CCSS's) is presented. The subdivision depth computation technique also includes distance evaluation techniques for CCSS patches with their control meshes. The distance and the subdivision depth computation techniques provide the long-needed precision/error control tools in subdivision surface trimming, finite element mesh generation, boolean operations, and surface tessellation for rendering processes.

Keywords: subdivision surfaces, distance evaluation, subdivision depth computation

1 Introduction

Subdivision surfaces have become popular recently in graphical modeling, animation and CAD/CAM because of their stability in numerical computation, simplicity in coding and, most importantly, their capability in modeling/representing complex shape of arbitrary topology. Given a control mesh and a set of *mesh refining rules* (or, more intuitively, *corner cutting rules*), one gets a *limit surface* by recursively cutting off corners of the control mesh [3][5]. The limit surface is called a *subdivision surface* because the corner cutting (mesh refining) process is a generalization of the uniform B-spline surface *subdivision technique*. Subdivision surfaces include uniform B-spline surfaces and piecewise Bézier surfaces as special cases. Actually subdivision surfaces include non-uniform B-spline surfaces and NURBS surfaces as special cases as well [10]. Subdivision surfaces can model/represent complex shape of arbitrary topology because there is no limit on the shape and topology of the control mesh of a subdivision surface. With the parametrization technique of subdivision surfaces becoming available [11], we now know that subdivision surfaces cover both *parametric forms* and *discrete forms*. Since parametric forms are good for design and representation and discrete forms are good for machining and tessellation (including FE mesh generation) [1], we finally have a representation scheme that is good for all graphics and CAD/CAM applications.

Research work for subdivision surfaces has been done in several important areas, such as surface trimming [7], boolean operations [2], and mesh editing [13]. However, the area of *precision/error control* for Catmull-Clark subdivision surfaces (CCSS's)is completely blank. For instance, given an error tolerance, how many levels of recursive Catmull-Clark subdivision should be performed on the initial control mesh so that the distance between the resultant control mesh and the limit surface would be less than the error tolerance? This error control technique is required in all tessellation based applications such as subdivision surface trimming, finite element mesh generation, boolean operations, and surface tessellation for rendering. A subdivision depth computation technique based on bounds of second derivatives has been presented for tensor product rational surfaces [4]. But nothing in this area has been done for Catmull-Clark subdivision surfaces yet. The technique used for tensor product rational surfaces can not be used here because the parameter space of a CCSS usually does not fit into a rectangular grid structure.

In this paper we will present a subdivision depth computation technique for a CCSS. The subdivision depth computation technique also includes distance evaluation techniques for a CCSS patch with its control mesh. The new techniques are based on the control points of the CCSS patch only and work for CCSS patches with or without an extraordinary vertex. The presented subdivision depth computation technique provides the first and an efficient error control tool that works for all tessellation based applications of CCSS's. A potential disadvantage of the subdivision depth computation technique is that it might generate a relatively large subdivision depth for a patch with an extraordinary vertex even though the patch is already flat enough. This is due to the fact that the first order norm can not measure the curvature difference between two points. A possible solution to this problem in given in the last section.

2 Subdivision Depth Computation for Patches not near an extraordinary vertex

Let $\mathbf{V}_0$, $\mathbf{V}_1$, $\mathbf{V}_2$ and $\mathbf{V}_3$ be the control points of a uniform cubic B-spline curve segment $\mathbf{C}(t)$ whose parameter space is $[0,1]$. If we parametrize the middle leg of the control polygon as follows: $\mathbf{L}(t) = \mathbf{V}_1 + (\mathbf{V}_2 - \mathbf{V}_1)t$, $0 \le t \le 1$, (see Figure 1) then the maximum of $\|\mathbf{L}(t) - \mathbf{C}(t)\|$ is called the *distance* between the curve segment and its control polygon. It is easy to see that

$$\begin{aligned}&\|\mathbf{L}(t) - \mathbf{C}(t)\| \\ &= \|\tfrac{(1-t)^3}{6}(2\mathbf{V}_1 - \mathbf{V}_0 - \mathbf{V}_2) + \tfrac{t^3}{6}(2\mathbf{V}_2 - \mathbf{V}_1 - \mathbf{V}_3)\| \\ &\le \tfrac{1}{6}\max\{\|2\mathbf{V}_1 - \mathbf{V}_0 - \mathbf{V}_2\|,\ \|2\mathbf{V}_2 - \mathbf{V}_1 - \mathbf{V}_3\|\}.\end{aligned} \tag{1}$$

Since $(2\mathbf{V}_1 - \mathbf{V}_0 - \mathbf{V}_2)/6$ and $(2\mathbf{V}_2 - \mathbf{V}_1 - \mathbf{V}_3)/6$ are the values of $\mathbf{L}(t) - \mathbf{C}(t)$ at $t = 0$ and $t = 1$, we have the following lemma.

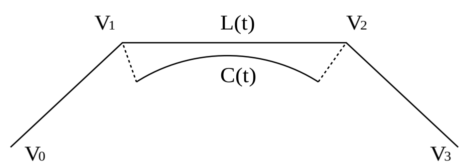

Figure 1: Definition of $\mathbf{L}(t)$.

Lemma 1: The maximum of $\|\mathbf{L}(t) - \mathbf{C}(t)\|$ occurs at the endpoints of the curve segment and can be expressed as

$$\begin{aligned}&\max_{0\le t\le 1} \|\mathbf{L}(t) - \mathbf{C}(t)\| \\ &= \tfrac{1}{6}\max\{\|2\mathbf{V}_1 - \mathbf{V}_0 - \mathbf{V}_2\|, \|2\mathbf{V}_2 - \mathbf{V}_1 - \mathbf{V}_3\|\}\end{aligned} \tag{2}$$

A form more general than (1) has been proved by Peters [8]. His result works for uniform B-spline curves of any degree. However, the above result is more intuitive and is all we need for subsequent results. We next define the *distance* between a uniform bicubic B-spline surface patch and its control mesh.

Let $\mathbf{V}_{i,j}$, $0 \le i,j \le 3$, be the control points of a uniform bicubic B-spline surface patch $\mathbf{S}(u,v)$ with parameter space $[0,1]\times[0,1]$. If we parametrize the central mesh face $\{\mathbf{V}_{1,1}, \mathbf{V}_{2,1}, \mathbf{V}_{1,2}, \mathbf{V}_{2,2}\}$ as follows:

$$\begin{aligned}\mathbf{L}(u,v) \;=\; &(1-v)[(1-u)\mathbf{V}_{1,1} + u\mathbf{V}_{2,1}] \\ &+v[(1-u)\mathbf{V}_{1,2} + u\mathbf{V}_{2,2}], \quad 0 \le u,v \le 1\end{aligned}$$

then the maximum of $\|\mathbf{L}(u,v) - \mathbf{S}(u,v)\|$ is called the *distance* between $\mathbf{S}(u,v)$ and its control mesh. If we define $\mathbf{Q}_{u,k}$, $\mathbf{Q}_{v,k}$, $\bar{\mathbf{Q}}_{u,k}$ and $\bar{\mathbf{Q}}_{v,k}$ as follows:

$$\begin{aligned}\mathbf{Q}_{u,k} &\equiv (1-u)\mathbf{V}_{1,k} + u\mathbf{V}_{2,k}, \\ \mathbf{Q}_{v,k} &\equiv (1-v)\mathbf{V}_{k,1} + v\mathbf{V}_{k,2}, \\ \bar{\mathbf{Q}}_{u,k} &\equiv \textstyle\sum_{i=0}^{3} N_{i,3}(u)\mathbf{V}_{i,k}, \\ \bar{\mathbf{Q}}_{v,k} &\equiv \textstyle\sum_{j=0}^{3} N_{j,3}(v)\mathbf{V}_{k,j}\end{aligned}$$

where $N_{i,3}(t)$ are standard uniform B-spline basis functions of degree three, we have

$$\begin{aligned}&\|\mathbf{L}(u,v) - \mathbf{S}(u,v)\| \\ &\le (1-v)\|\mathbf{Q}_{u,1} - \bar{\mathbf{Q}}_{u,1}\| + v\|\mathbf{Q}_{u,2} - \bar{\mathbf{Q}}_{u,2}\| \\ &\quad + \sum_{i=0}^{3} N_{i,3}(u)\|\mathbf{Q}_{v,i} - \bar{\mathbf{Q}}_{v,i}\|.\end{aligned}$$

By applying Lemma 1 on $\|\mathbf{Q}_{u,1} - \bar{\mathbf{Q}}_{u,1}\|$, $\|\mathbf{Q}_{u,2} - \bar{\mathbf{Q}}_{u,2}\|$ and $\|\mathbf{Q}_{v,i} - \bar{\mathbf{Q}}_{v,i}\|$, $i = 1,2,3$, and by defining M^0 as the maximum norm of the second order forward differences of the control points of $\mathbf{S}(u,v)$, we have

$$\begin{aligned}\|\mathbf{L}(u,v) - \mathbf{S}(u,v)\| &\le \tfrac{1}{6}[(1-v)M^0 + vM^0 \\ &+ \textstyle\sum_{i=0}^{3} N_{i,3}(u)M^0] \le \tfrac{1}{3}M^0.\end{aligned}$$

M^0 is called the *second order norm* of $\mathbf{S}(u,v)$. This leads to the following lemma.

Lemma 2: The maximum of $\|\mathbf{L}(u,v) - \mathbf{S}(u,v)\|$ satisfies the following inequality

$$\max_{0\le u,v\le 1} \|\mathbf{L}(u,v) - \mathbf{S}(u,v)\| \le \frac{1}{3}M^0 \tag{3}$$

where M^0 is the second order norm of $\mathbf{S}(u,v)$.

Note that even though the maximum of $\|\mathbf{L}(t) - \mathbf{C}(t)\|$ occurs at the end points of the curve segment $\mathbf{C}(t)$, the maximum of $\|\mathbf{L}(u,v) - \mathbf{S}(u,v)\|$ for a surface patch usually does not occur at the corners of $\mathbf{S}(u,v)$. In the following, we present subdivision depth computation technique for CCSS patches not adjacent to an extraordinary vertex.

Let $\mathbf{V}_{i,j}$, $0 \le i,j \le 3$, be the control points of a uniform bicubic B-spline surface patch $\mathbf{S}(u,v)$. We use $\mathbf{V}^k_{i,j}$, $0 \le i,j \le 3 + 2^k - 1$, to represent the new control points of the surface patch after k levels of recursive subdivision. The indexing of the new control points follows the convention that $\mathbf{V}^k_{0,0}$ is always the *face point* of the mesh face $\{\mathbf{V}^{k-1}_{0,0}, \mathbf{V}^{k-1}_{1,0}, \mathbf{V}^{k-1}_{0,1}, \mathbf{V}^{k-1}_{1,1}\}$. The new control points $\mathbf{V}^k_{i,j}$ will be called the *level-k control points* of $\mathbf{S}(u,v)$ and the new control mesh will be called the *level-k control mesh* of $\mathbf{S}(u,v)$.

Note that if we divide the parameter space of the surface patch into 4^k regions as follows:

$$\Omega^k_{m,n} = [\frac{m}{2^k}, \frac{m+1}{2^k}] \times [\frac{n}{2^k}, \frac{n+1}{2^k}], \tag{4}$$

where $0 \leq m,n \leq 2^k - 1$ and let the corresponding subpatches be denoted $\mathbf{S}^k_{m,n}(u,v)$, then each $\mathbf{S}^k_{m,n}(u,v)$ is a uniform bicubic B-spline surface patch defined by the level-k control point set $\{\mathbf{V}^k_{p,q} \mid m \leq p \leq m+3, n \leq q \leq n+3\}$. $\mathbf{S}^k_{m,n}(u,v)$ is called a *level-k subpatch* of $\mathbf{S}(u,v)$. One can define a level-k bilinear plane $\mathbf{L}^k_{m,n}$ on $\{\mathbf{V}^k_{p,q} \mid p = m+1, m+2; q = n+1, n+2\}$ and measure the distance between $\mathbf{L}^k_{m,n}(u,v)$ and $\mathbf{S}^k_{m,n}(u,v)$. We say that the *distance between* $\mathbf{S}(u,v)$ *and the level-k control mesh is smaller than* ϵ if the distance between each level-k subpatch $\mathbf{S}^k_{m,n}(u,v)$ and the corresponding level-k bilinear plane $\mathbf{L}^k_{m,n}(u,v)$, $0 \leq m,n \leq 2^k - 1$, is smaller than ϵ. In the following, we will show how to compute a subdivision depth k for a given ϵ so that the distance between $\mathbf{S}(u,v)$ and the level-k control mesh is smaller than ϵ after k levels of recursive subdivision. The following lemma is needed in the derivation of the computation process. If we use $M^k_{m,n}$ to represent the second order norm of $\mathbf{S}^k_{m,n}(u,v)$, i.e., the maximum norm of the second order forward differences of the control points of $\mathbf{S}^k_{m,n}(u,v)$, then the lemma shows the second order norm of $\mathbf{S}^k_{m,n}(u,v)$ converges at a rate of $1/4$ of the level-$(k-1)$ second order norm. The proof of this lemma is given in Appendix A.

Lemma 3 If $M^k_{m,n}$ is the second order norm of $\mathbf{S}^k_{m,n}(u,v)$ then we have

$$M^k_{m,n} \leq \left(\frac{1}{4}\right)^k M^0 \tag{5}$$

where M^0 is the second order norm of $\mathbf{S}(u,v)$.

With Lemmas 2 and 3, it is easy to see that, for any $0 \leq m,n \leq 2^{k-1}$, we have

$$\begin{aligned} \max_{0 \leq u,v \leq 1} & \|\mathbf{L}^k_{m,n}(u,v) - \mathbf{S}^k_{m,n}(u,v)\| \\ & \leq \tfrac{1}{3} M^k_{m,n} \leq \tfrac{1}{3}\left(\tfrac{1}{4}\right)^k M^0. \end{aligned} \tag{6}$$

Hence, if k is large enough to make the right side of (6) smaller than ϵ, we have

$$\max_{0 \leq u,v \leq 1} \|\mathbf{L}^k_{m,n}(u,v) - \mathbf{S}^k_{m,n}(u,v)\| \leq \epsilon$$

for every $0 \leq m,n \leq 2^{k-1}$. This leads to the following main result of this subsection.

Theorem 4 Let $\mathbf{V}_{i,j}$, $0 \leq i,j \leq 3$, be the control points of a uniform bicubic B-spline surface patch $\mathbf{S}(u,v)$. For any given $\epsilon > 0$, if

$$k \geq \lceil \log_4\left(\frac{M^0}{3\epsilon}\right) \rceil \tag{7}$$

levels of recursive subdivision are performed on the control points of $\mathbf{S}(u,v)$ then the distance between $\mathbf{S}(u,v)$ and the level-k control mesh is smaller than ϵ where M^0 is the second order norm of $\mathbf{S}(u,v)$.

3 Subdivision Depth Computation for Patches near an extraordinary vertex

The subdivision depth computation process for a CCSS patch near an extraordinary vertex is different. This is because in the vicinity of an extraordinary vertex one does not have a uniform B-spline surface patch representation and, consequently, cannot use the technique of Theorem 4 directly. Fortunately, the size of such a vicinity can be made as small as possible, therefore, one can reduce the size of such a vicinity to a degree that is tolerable (i.e., within the given error bound) and use the technique of Theorem 4 to work on the remaining part of the surface patch. A subdivision depth computation technique based on this concept for a CCSS patch near an extraordinary vertex will be presented below. we assume the initial mesh has been subdivided at least twice so that each mesh face is a quadrilateral and contains at most one extraordinary vertex. We need to define a few notations first.

Let $\Pi^0_0 = \{ \mathbf{V}_i \mid 1 \leq i \leq 2N+8 \}$ be a level-0 control point set that influences the shape of a surface patch $\mathbf{S}(u,v)$ $(= \mathbf{S}^0_0(u,v))$. $\mathbf{V}_1$ is an *extraordinary vertex* with *valence N*. The control vertices are ordered following Stam's fashion [11] (see Figure 2).

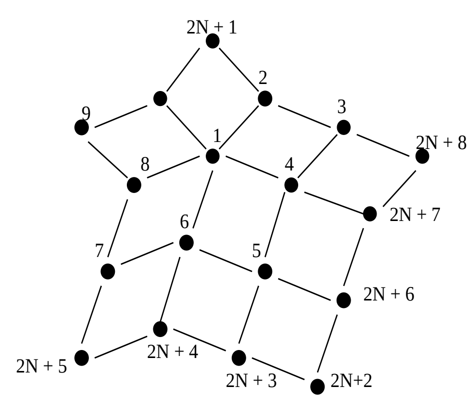

Figure 2: Ordering of control points for a CCSS patch with an extraordinary vertex.

If we use $\mathbf{V}^n_i$ to represent the level-n control vertices generated after n levels of recursive Catmull-Clark subdivision, and use $\mathbf{S}^n_0$, $\mathbf{S}^n_1$, $\mathbf{S}^n_2$ and $\mathbf{S}^n_3$ to represent the subpatches of $\mathbf{S}^{n-1}_0$ defined over the tiles

$$\begin{aligned} \Omega^n_0 &= [0, \tfrac{1}{2^n}] \times [0, \tfrac{1}{2^n}], \\ \Omega^n_1 &= [\tfrac{1}{2^n}, \tfrac{1}{2^{n-1}}] \times [0, \tfrac{1}{2^n}], \\ \Omega^n_2 &= [\tfrac{1}{2^n}, \tfrac{1}{2^{n-1}}] \times [\tfrac{1}{2^n}, \tfrac{1}{2^{n-1}}], \\ \Omega^n_3 &= [0, \tfrac{1}{2^n}] \times [\tfrac{1}{2^n}, \tfrac{1}{2^{n-1}}], \end{aligned}$$

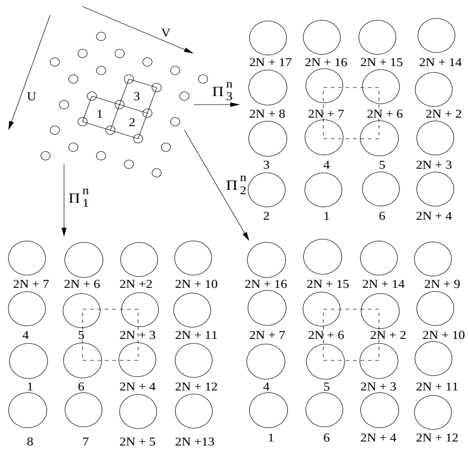

Figure 3: Control point sets Π_1^n, Π_2^n and Π_3^n.

respectively, then the shape of $\mathbf{S}_0^n$, $\mathbf{S}_1^n$, $\mathbf{S}_2^n$ and $\mathbf{S}_3^n$ are influenced by the level-n control point sets Π_0^n, Π_1^n, Π_2^n and Π_3^n, respectively. Π_0^n is defined below and definition of Π_1^n, Π_2^n and Π_3^n can be found in Figure 3.

$$\Pi_0^n = \{ \ \mathbf{V}_i^n \mid 1 \le i \le 2N+8 \ \}$$

$\mathbf{S}_1^n$, $\mathbf{S}_2^n$ and $\mathbf{S}_3^n$ are standard uniform bicubic B-spline surface patches because their control meshes satisfy a 4-by-4 structure. Hence, the technique described in Theorem 4 can be used to compute a subdivision depth for each of them. $\mathbf{S}_0^n$ is not a standard uniform bicubic B-spline surface patch. Hence, Theorem 4 can not be used to compute a subdivision depth for $\mathbf{S}_0^n$ directly. For the convenience of reference, we shall call $\mathbf{S}_0^n$ a *level-n extraordinary subpatch* of $\mathbf{S}(u,v)$ because it contains the limit point of the extraordinary points.[1] Note that if $\mathbf{H}_0$ and $\mathbf{H}_n$ are column vector representations of the control points of Π_0^0 and Π_0^n, respectively,

$$\begin{array}{rcl} \mathbf{H}_0 & \equiv & (\mathbf{V}_0, \mathbf{V}_1, \cdots, \mathbf{V}_{2N+8})^t, \\ \mathbf{H}_n & \equiv & (\mathbf{V}_0^n, \mathbf{V}_1^n, \cdots, \mathbf{V}_{2N+8}^n)^t \end{array}$$

where $(\mathbf{X},\ \mathbf{X}, \cdots, \mathbf{X})^t$ represents the transpose of the row vector $(\mathbf{X},\ \mathbf{X}, \cdots, \mathbf{X})$ then we have

$$\mathbf{H}_n = (T)^n \ \mathbf{H}_0 \tag{8}$$

where T is the $(2N{+}8)\times(2N{+}8)$ (extended) subdivision matrix defined as follows [6][11]:

$$T \equiv \begin{pmatrix} \bar{T} & \mathbf{0} \\ \bar{T}_{1,1} & \bar{T}_{1,2} \end{pmatrix}, \tag{9}$$

[1] To be proved in the next subsection.

with

$$\bar{T} = \begin{pmatrix} a_N & b_N & c_N & b_N & c_N & b_N & \cdots & b_N & c_N \\ d & d & e & e & 0 & 0 & \cdots & e & e \\ f & f & f & f & 0 & 0 & \cdots & 0 & 0 \\ d & e & e & d & e & e & \cdots & 0 & 0 \\ f & 0 & 0 & f & f & f & \cdots & 0 & 0 \\ & & \vdots & & & & \ddots & \vdots & \\ d & e & 0 & 0 & 0 & 0 & \cdots & d & e \\ f & f & 0 & 0 & 0 & 0 & \cdots & f & f \end{pmatrix}, \tag{10}$$

$$\bar{T}_{1,1} = \begin{pmatrix} c & 0 & 0 & b & a & b & 0 & 0 & \mathbf{0} \\ e & 0 & 0 & e & d & d & 0 & 0 & \mathbf{0} \\ b & 0 & 0 & c & b & a & b & c & \mathbf{0} \\ e & 0 & 0 & 0 & 0 & d & d & e & \mathbf{0} \\ e & 0 & 0 & d & d & e & 0 & 0 & \mathbf{0} \\ b & c & b & a & b & c & 0 & 0 & \mathbf{0} \\ e & e & d & d & 0 & 0 & 0 & 0 & \mathbf{0} \end{pmatrix}, \tag{11}$$

$$\bar{T}_{1,2} = \begin{pmatrix} c & b & c & 0 & b & c & 0 \\ 0 & e & e & 0 & 0 & 0 & 0 \\ 0 & c & b & c & 0 & 0 & 0 \\ 0 & 0 & e & e & 0 & 0 & 0 \\ 0 & 0 & 0 & 0 & e & e & 0 \\ 0 & 0 & 0 & 0 & c & b & c \\ 0 & 0 & 0 & 0 & 0 & e & e \end{pmatrix} \tag{12}$$

and

$$\begin{array}{c} a_N = 1 - \frac{7}{4N}, b_N = \frac{3}{2N^2}, c_N = \frac{1}{4N^2}, a = \frac{9}{16}, \\ b = \frac{3}{32}, c = \frac{1}{64}, d = \frac{3}{8}, e = \frac{1}{16}, f = \frac{1}{4}. \end{array}$$

3.1 Computing subdivision depth for a vicinity of the extraordinary vertex

The goal here is to find an integer n_ϵ for a given $\epsilon > 0$ so that if n $(\ge n_\epsilon)$ recursive subdivisions are performed on Π_0^0, then the control point set of the level-n extraordinary subpatch $\mathbf{S}_0^n$ of $\mathbf{S}(u,v)$, $\Pi_0^n = \{ \ \mathbf{V}_i^n \mid 1 \le i \le 2N+8 \ \}$, is contained in the sphere $B(\mathbf{V}_5^{n+1},\ \epsilon/2)$ with center $\mathbf{V}_5^{n+1} \equiv (\mathbf{V}_1^n + \mathbf{V}_4^n + \mathbf{V}_5^n + \mathbf{V}_6^n)/4$ and radius $\epsilon/2$. Note that if the $(2N+8)$-point control mesh Π_0^n is contained in the sphere $B(\mathbf{V}_5^{n+1},\ \epsilon/2)$ then the level-n extraordinary subpatch $\mathbf{S}_0^n$ is contained in the sphere $B(\mathbf{V}_5^{n+1},\ \epsilon/2)$ as well. This follows from the fact that $\mathbf{S}_0^n$, as the limit surface of Π_0^n, is contained in the *convex hull* of Π_0^n and the convex hull of Π_0^n is contained in the sphere $B(\mathbf{V}_5^{n+1},\ \epsilon/2)$. But then we have

$$\max \|\mathbf{S}_0^n(u,v) - \mathbf{L}_0^n(u,v)\| < \epsilon \tag{13}$$

where $\mathbf{L}_0^n(u,v)$ is a bilinear plane defined on the level-n mesh face $\{ \ \mathbf{V}_1^n,\ \mathbf{V}_4^n,\ \mathbf{V}_5^n,\ \mathbf{V}_6^n \ \}$. The construction of such an n_ϵ depends on several properties of the (extended) subdivision matrix T and the control point sets $\{\Pi_0^n\}$.

First note that since all the entries of the extended subdivision matrix T are non-negative and the sum of each row equals one, the extended subdivision matrix is a *transition probability matrix* of a $(2N+8)$-state Markov chain [9]. In particular, the $(2N+1)\times(2N+1)$ block $\bar{T}$ of T is a *transition probability matrix* of a $(2N+1)$-state Markov chain. The entries in the first row and first column of $\bar{T}$ are all non-zero. Therefore, the matrix $\bar{T}$ is *irreducible* because $(\bar{T})^2$ has no zero entries and, consequently, all the states are accessible to each other. On the other hand, since all the diagonal entries of $\bar{T}$ are non-zero and entries of $(\bar{T})^n$ are non-zero for all $n \ge 2$, it follows that all the states of $\bar{T}$ are *aperiodic* and *positive recurrent*. Consequently, the Markov chain is *irreducible* and *ergodic*. By the well-known theorem of Markov chain ([9], Theorem 4.1), $(\bar{T})^n$ converges to a limit matrix $\bar{T}^*$ whose rows are identical. More precisely,

$$\lim_{n\to\infty}(\bar{T})^n = \bar{T}^* \equiv \begin{pmatrix} \Delta_1 & \Delta_2 & \cdots & \Delta_{2N+1} \\ \Delta_1 & \Delta_2 & \cdots & \Delta_{2N+1} \\ \vdots & \vdots & \ddots & \vdots \\ \Delta_1 & \Delta_2 & \cdots & \Delta_{2N+1} \end{pmatrix} \tag{14}$$

where Δ_i are the unique non-negative solution of

$$\begin{aligned} &\Delta_j = \textstyle\sum_{i=1}^{2N+1} \Delta_i \bar{t}_{i,j}, \qquad j = 1,2,\cdots,2N+1 \\ &\textstyle\sum_{j=1}^{2N+1} \Delta_j = 1 \end{aligned} \tag{15}$$

with $\bar{t}_{i,j}$ being the entries of $\bar{T}$. One can easily get the following observations.

- The vector $(\Delta_1, \Delta_2, \cdots, \Delta_{2N+1})$ satisfies the following properties:

  $$\begin{aligned} &\Delta_1 = \tfrac{N}{N+5} \\ &\Delta_2 = \Delta_4 = \cdots = \Delta_{2N} = \tfrac{4}{N(N+5)} \\ &\Delta_3 = \Delta_5 = \cdots = \Delta_{2N+1} = \tfrac{1}{N(N+5)} \end{aligned}$$

- The matrix $\bar{T}^*$ is an idempotent matrix, i.e., $\bar{T}^*\bar{T}^* = \bar{T}^*$. Hence, $\bar{T}^*$ has two eigenvalues, 1 and 0 (with multiplicity $2N$).

- $\bar{T}$ has 1 as an eigenvalue and all the other $2N$ eigenvalues of $\bar{T}$ have a magnitude smaller than one.

- As it is well known [6], the limit point of $\{\mathbf{V}_1^n\}$ is

  $$\mathbf{V}_1^* \equiv \Delta_1\mathbf{V}_1 + \Delta_2\mathbf{V}_2 + \cdots + \Delta_{2N+1}\mathbf{V}_{2N+1}.$$

  But $\mathbf{V}_1^*$ is actually the limit point of all $\mathbf{V}_j^n$, $j = 1,2,\cdots,2N+8$. Therefore, the convex hull of $\{\mathbf{V}_1^n,\ \mathbf{V}_2^n,\cdots,\ \mathbf{V}_{2N+8}^n\}$ converges to $\mathbf{V}_1^*$ when n tends to infinity and, consequently, $\mathbf{V}_1^* = \mathbf{S}(0,0)$. The fact that $\mathbf{V}_1^*$ is the limit point of $\{\mathbf{V}_1^n, \mathbf{V}_2^n, \cdots, \mathbf{V}_{2N+1}^n\}$ follows from (8) and (14). The fact that $\mathbf{V}_1^*$ is also the limit point of $\{\mathbf{V}_{2N+2}^n, \mathbf{V}_{2N+3}^n, \cdots, \mathbf{V}_{2N+8}^n\}$ is proved in Appendix B.

The last observation is important because it shows that

$$\max_{\mathbf{V}\in\Pi_0^n} \|\mathbf{V}_5^{n+1} - \mathbf{V}\| \tag{16}$$

converges. Therefore, it is possible to reduce the size of $\mathbf{S}_0^n$ to a degree that is tolerable if n is large enough. For a given $\epsilon > 0$ we will find an n_ϵ so that if $n \ge n_\epsilon$ then the level-n control point set Π_0^n is contained in the sphere $B(\mathbf{V}_5^{n+1},\ \epsilon/2)$. To do this, we need to know how fast (16) converges.

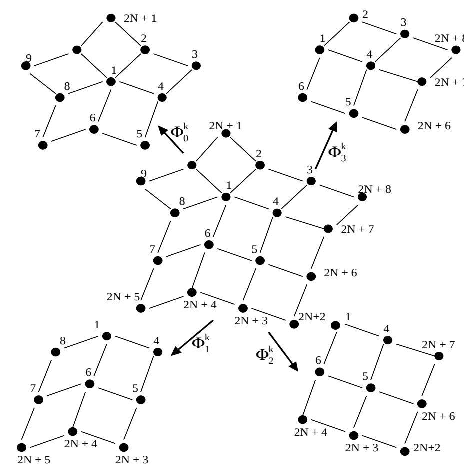

Figure 4: Control point sets Φ_0^n, Φ_1^n, Φ_2^n and Φ_3^n.

Let Φ_0^k, Φ_1^k, Φ_2^k and Φ_3^k be subsets of Π_0^k defined as follows (see Figure 4):

$$\begin{array}{lcl} \Phi_0^k &=& \{\mathbf{V}_j^k \mid j = 1,2,\cdots,2N+1\}, \\ \Phi_1^k &=& \{\mathbf{V}_j^k \mid j = 1,4,5,\cdots,8,2N+3,2N+4, \\ && \quad 2N+5\}, \\ \Phi_2^k &=& \{\mathbf{V}_j^k \mid j = 1,4,5,6,2N+2,2N+3, \\ && \quad 2N+4,2N+6,2N+7\}, \\ \Phi_3^k &=& \{\mathbf{V}_j^k \mid j = 1,2,\cdots,6,2N+6,2N+7, \\ && \quad 2N+8\} \end{array} \tag{17}$$

($\mathbf{V}_8^k$ in Φ_1^k should be replaced with $\mathbf{V}_2^k$ if $N=3$) and define G_0^k, G_1^k, G_2^k and G_3^k as follows:

$$\begin{array}{lcl} G_0^k &=& \max_{\mathbf{V}\in\Phi_0^k} \|\mathbf{V}_1^k - \mathbf{V}\|, \\ G_1^k &=& \max_{\mathbf{V}\in\Phi_1^k} \|\mathbf{V}_6^k - \mathbf{V}\|, \\ G_2^k &=& \max_{\mathbf{V}\in\Phi_2^k} \|\mathbf{V}_5^k - \mathbf{V}\|, \\ G_3^k &=& \max_{\mathbf{V}\in\Phi_3^k} \|\mathbf{V}_4^k - \mathbf{V}\|. \end{array} \tag{18}$$

G_i^k is called the *first order norm* of Φ_i^k, $i = 0,1,2,3$. We need the following lemma for the construction of n_ϵ. The proof is shown in Appendix C.

<u>Lemma 5</u> If Φ_i^k and G_i^k are defined as above then, for $i = 0,1,2,3$, we have

$$G_i^k \le \begin{cases} \left(\frac{3}{4}\right)^k G^0, & \text{if } N = 3 \\ \left(\frac{3}{4} + \frac{7}{4N} - \frac{13}{2N^2}\right)^k G^0, & \text{if } N \ge 5 \end{cases} \tag{19}$$

where $G^0 \equiv \max\{G_0^0,\ G_1^0,\ G_2^0,\ G_3^0\}$. G^0 is called the *first order norm* of Π_0^0.

To construct n_ϵ, note that if $\mathbf{V} \in \Pi_0^n$ and $\mathbf{V} \in \Phi_0^n$, we have

$$\begin{aligned}\|\mathbf{V}_5^{n+1} - \mathbf{V}\| &\leq \tfrac{1}{4}\|\mathbf{V}_4^n - \mathbf{V}_1^n\| + \tfrac{1}{4}\|\mathbf{V}_5^n - \mathbf{V}_1^n\| \\ &\quad + \tfrac{1}{4}\|\mathbf{V}_6^n - \mathbf{V}_1^n\| + \|\mathbf{V}_1^n - \mathbf{V}\| \leq \tfrac{7}{4}G_0^n.\end{aligned}$$

It is easy to prove that similar inequalities hold for Φ_1^n, Φ_2^n and Φ_3^n as well. Hence, for each $\mathbf{V} \in \Pi_0^n$, by Lemma 5, we have

$$\|\mathbf{V}_5^{n+1} - \mathbf{V}\| \leq \begin{cases} \frac{7}{4}\left(\frac{3}{4}\right)^n G^0, & \text{if } N = 3 \\ \frac{7}{4}\left(\frac{3}{4} + \frac{7}{4N} - \frac{13}{2N^2}\right)^n G^0, & \text{if } N \geq 5 \end{cases} \tag{20}$$

Since the maximum of $\frac{3}{4} + \frac{7}{4N} - \frac{13}{2N^2}$ occurs at $N = 7$, (20) can be simplified as

$$\|\mathbf{V}_5^{n+1} - \mathbf{V}\| \leq \frac{7}{4}\left(\frac{1}{\delta}\right)^n G^0 \tag{21}$$

where

$$\delta = \begin{cases} \frac{4}{3}, & \text{if } N = 3 \\ \frac{98}{85}, & \text{if } N \geq 5 \end{cases}. \tag{22}$$

Hence, $\|\mathbf{V}_5^{n+1} - \mathbf{V}\|$ is smaller than $\epsilon/2$ if n is large enough to make the right hand side of (21) smaller than or equal to $\epsilon/2$. Consequently, we have the following theorem.

__Theorem 6__ Let $\Pi_0^0 = \{\mathbf{V}_i \mid 1 \leq i \leq 2N+8\}$ be a level-0 control point set that influences the shape of a CCSS patch $\mathbf{S}(u,v)$ $(= \mathbf{S}_0^0(u,v))$. $\mathbf{V}_1$ is an extraordinary vertex with *valence* N. The control vertices are ordered following Stam's fashion [11] (see Figure 2). For a given $\epsilon > 0$, if n_ϵ is defined as follows:

$$n_\epsilon \equiv \lceil \log_\delta \left(\frac{7G^0}{2\epsilon}\right) \rceil, \qquad \delta = \begin{cases} \frac{4}{3}, & \text{if } N = 3 \\ \frac{98}{85}, & \text{if } N \geq 5 \end{cases} \tag{23}$$

where G^0 is the first order norm of Π_0^0, then the distance between the level-n extraordinary subpatch $\mathbf{S}_0^n(u,v)$ and the corresponding bilinear plane $\mathbf{L}_0^n(u,v)$ is smaller than or equal to ϵ if $n \geq n_\epsilon$.

Theorem 6 shows that the rate of convergence of the control mesh in the vicinity of an extraordinary vertex is fastest when valence of the extraordinary vertex is three.

3.2 Computing subdivision depth for the remaining part

The idea here is, for each k between 1 and n_ϵ, to determine a subdivision depth D_k $(\geq n_\epsilon)$ so that if D_k recursive subdivisions are performed on the control mesh Π_0^0 of $\mathbf{S}(u,v)$, then the distance between the level-D_k control mesh and the subpatches $\mathbf{S}_i^k$, $i = 1,2,3$, is smaller than ϵ. Consequently, if we define D to be the maximum of these D_k (i.e., $D = \max\{D_k | 1 \leq k \leq n_\epsilon\}$), then after D recursive subdivisions, the distance between the level-D control mesh and the subpatches $\mathbf{S}_i^k$, $i = 1,2,3$, would be smaller than ϵ for all $1 \leq k \leq n_\epsilon$. Note that the distance between the level-D control mesh and the subpatches $\mathbf{S}_1^k$, $\mathbf{S}_2^k$ and $\mathbf{S}_3^k$ for $n_\epsilon + 1 \leq k \leq D$, and the distance between the level-D control mesh and the level-D extraordinary subpatch $\mathbf{S}_0^D$ would be smaller than ϵ as well. This is because these subpatches are subpatches of $\mathbf{S}_0^{n_\epsilon}$ and the distance between $\mathbf{S}_0^{n_\epsilon}$ and the level-n_ϵ control mesh is already smaller than ϵ. Hence, the key here is the construction of D_k. We will show the construction of D_k for $\mathbf{S}_3^k(u,v)$. This D_k works for $\mathbf{S}_1^k(u,v)$ and $\mathbf{S}_2^k(u,v)$ as well.

For $0 \leq u,v \leq 1$, define a bilinear plane $\mathbf{L}_3^k(u,v)$ on the mesh face $\{\mathbf{V}_4^k, \mathbf{V}_5^k, \mathbf{V}_{2N+7}^k, \mathbf{V}_{2N+6}^k\}$ as follows:

$$\begin{aligned}\mathbf{L}_3^k(u,v) &= (1-v)[(1-u)\mathbf{V}_4^k + u\mathbf{V}_5^k] \\ &\quad + v[(1-u)\mathbf{V}_{2N+7}^k + u\mathbf{V}_{2N+6}^k].\end{aligned} \tag{24}$$

Since $\mathbf{S}_3^k(u,v)$ is a uniform bicubic B-spline surface patch with control mesh Π_3^k, we have, by Lemma 2,

$$\|\mathbf{L}_3^k(u,v) - \mathbf{S}_3^k(u,v)\| \leq \frac{1}{3}Z_3^k \tag{25}$$

where Z_3^k is the second order norm of $\mathbf{S}_3^k(u,v)$. If we define Z_0^i to be the second order norm of $\mathbf{S}_0^i(u,v)$, we have

$$Z_3^k \leq W Z_0^{k-1} \leq (W)^k Z_0^0 \tag{26}$$

where

$$W = \begin{cases} \frac{2}{3}, & \text{if } N = 3 \\ \frac{1}{2} + \frac{1}{4N} + \frac{21}{4N^2}, & \text{if } N = 5 \\ \frac{3}{4} + \frac{2}{N} - \frac{21}{2N^2}, & \text{if } N > 5 \end{cases}. \tag{27}$$

The proof of (26) is shown in Appendix D. Hence, by combining the above results, we have

__Lemma 7__ The maximum distance between $\mathbf{S}_3^k$ and $\mathbf{L}_3^k$ satisfies the following inequality

$$\max \|\mathbf{L}_3^k(u,v) - \mathbf{S}_3^k(u,v)\| \leq \frac{1}{3}(W)^k Z_0^0 \tag{28}$$

where W is defined in (27) and Z_0^0 is the second order norm of $\mathbf{S}(u,v)$.

It should be pointed out that when defining Z_0^i, only the following items are needed for second order forward differences involving $\mathbf{V}_1^i$:

$$\|2\mathbf{V}_1^i - \mathbf{V}_{2j}^i - \mathbf{V}_{2[(j+2)\%N]}^i\|, \qquad j = 1,2,\cdots,N.$$

Lemma 7 shows that if $\frac{1}{3}(W)^k Z_0^0 \leq \epsilon$ then the distance between $\mathbf{S}_3^k$ and $\mathbf{L}_3^k$ is already smaller than ϵ. However, since n_ϵ subdivisions have to be performed on Π_0^0 to get $\mathbf{S}_0^{n_\epsilon}$ anyway, D_k for $\mathbf{S}_3^k$ in this case is set to n_ϵ. This condition holds for $\mathbf{S}_1^k$ and $\mathbf{S}_2^k$ as well.

If $\frac{1}{3}(W)^k Z_0^0 > \epsilon$, further subdivisions are needed on Π_i^k, $i = 1, 2, 3$, to make the distance between $\mathbf{S}_i^k$, $i = 1, 2, 3$, and the corresponding mesh faces smaller than ϵ. Consider $\mathbf{S}_3^k$ again. $\mathbf{S}_3^k$ is a uniform bicubic B-spline surface patch with control mesh Π_3^k. Therefore, if l_k recursive subdivisions are performed on the control mesh Π_3^k, by Lemma 2 and Lemma 3, we would have

$$\|\mathbf{L}_3^{l_k}(u,v) - \mathbf{S}_3^k(u,v)\| \leq \frac{1}{3}(\frac{1}{4})^{l_k} Z_3^k \tag{29}$$

where $\mathbf{L}_3^{l_k}(u,v)$ is a level-l_k control mesh relative to Π_3^k and Z_3^k is the second order norm of $\mathbf{S}_3^k(u,v)$. Therefore, by combining the above result with (26), we have

$$\|\mathbf{L}_3^{l_k}(u,v) - \mathbf{S}_3^k(u,v)\| \leq \frac{1}{3}(\frac{1}{4})^{l_k}(W)^k Z_0^0. \tag{30}$$

We get the following Lemma by setting the right hand side of (30) smaller than or equal to ϵ.

Lemma 8 In Lemma 7, if the distance between $\mathbf{S}_3^k$ and $\mathbf{L}_3^k$ is not smaller than ϵ, then one needs to perform l_k

$$l_k = \lceil \log_4 \left(\frac{(W)^k Z_0^0}{3\epsilon} \right) \rceil \tag{31}$$

more recursive subdivisions on the level-k control mesh Π_3^k of $\mathbf{S}_3^k$ to make the distance between $\mathbf{S}_3^k$ and the level-$(k + l_k)$ control mesh smaller than ϵ.

This result works for $\mathbf{S}_1^k$ and $\mathbf{S}_2^k$ as well. Note that the value of $(W)^k Z_0^0$ is already computed in Lemma 7 and W has to be computed only once. Therefore, the subdivision depth D_k for $\mathbf{S}_1^k$, $\mathbf{S}_2^k$ and $\mathbf{S}_3^k$ is defined as follows:

$$D_k = max\{n_\epsilon,\ k + \lceil \log_4 \left(\frac{(W)^k Z_0^0}{3\epsilon} \right) \rceil\} \tag{32}$$

Consequently, we have the following main theorem:

Theorem 9 Let $\Pi_0^0 = \{\ \mathbf{V}_i |\ 1 \leq i \leq 2N + 8\}$ be the control mesh of a CCSS patch $\mathbf{S}(u,v)$. The control points are ordered following Stam's fashion [11] with $\mathbf{V}_1$ being an extraordinary vertex of valence N (see Figure 2). For a given $\epsilon > 0$, if we compute n_ϵ as in (23) and D as follows:

$$D = max\{D_k | 1 \leq k \leq n_\epsilon\} \tag{33}$$

where D_k is defined in (32) then after D recursive subdivisions, the distance between $\mathbf{S}(u,v)$ and the level-D control mesh is smaller than ϵ.

4 Examples

Some examples of the presented distance evaluating and subdivision depth computing techniques are shown in this section. In Figures 5(a), 5(b) and 5(c), the distances between the blue faces of the control meshes and the corresponding limit surface patches are 0.034, 0.15 and 0.25, respectively. For an error tolerance of 0.01, the subdivision depths computed for these mesh faces are 1, 22 and 24, respectively. The reason that the last two cases have large subdivision depths is because each of them has an extraordinary vertex. For the blue mesh face shown in Figure 5(c), subdivision depths for error tolerances 0.25, 0.2, 0.1, 0.01, 0.001, and 0.0001 are 1, 3, 9, 24, 40, and 56, respectively.

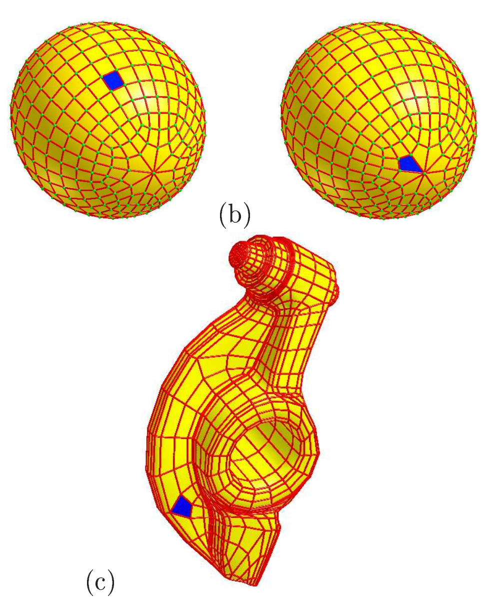

(a) (b) (c)

Figure 5: Distance and subdivision depth computation for a CCSS patch with: (a) no extraordinary vertex, (b) an extraordinary vertex of valence 8, (c) an extraordinary vertex of valence 5.

5 Conclusions

A subdivision depth computation technique for CCSS's is presented. This technique provides a precision/error control tool for all tessellation based applications of subdivision surfaces.

One possible disadvantage of the subdivision depth computation technique is that it might generate a relatively large subdivision depth for a vicinity of an extraordinary vertex which is actually quite flat. This is because the first order norm can detect the location difference of two points, but not the difference between their curvatures. Therefore, even though two points are on the same plane, as far as they are far apart, a large n_ϵ would still be generated by the subdivision depth computation process (see Theorem 6). A possible solution to this problem is to consider second order norm for Φ_0^n, Φ_1^n, Φ_2^n and Φ_3^n as well as the first order norm when computing n_ϵ for the vicinity of an extraordinary vertex.

6 Appendix A: Proof of Lemma 3

It is sufficient to show that, for each positive integer i, one has

$$M_{0,0}^{i+1} \le \frac{1}{4} M_{0,0}^i. \tag{34}$$

The sixteen second order forward differences involved in $M_{0,0}^{i+1}$ can be classified into four dategories: (C-1) $F-E-F$, (C-2) $E-F-E$, (C-3) $E-V-E$, and (C-4) $V-E-V$, based on the type of the vertices. For instance, a second order forward difference is said to be in the first category if an *edge vertex* is sandwished by two *face vertices*, such as $2\mathbf{V}_{1,0}^{i+1} - \mathbf{V}_{0,0}^{i+1} - \mathbf{V}_{2,0}^{i+1}$. Each category consists of four second order forward differences. We need to show that all these categories satisfy (34). In the following, we prove (34) for one item of each category. The proof of the other items is similar.

Case 1 ($F-E-F$): consider $2\mathbf{V}_{0,1}^{i+1} - \mathbf{V}_{0,2}^{i+1} - \mathbf{V}_{0,0}^{i+1}$.

$$\begin{aligned}
&\|2\mathbf{V}_{0,1}^{i+1} - \mathbf{V}_{0,2}^{i+1} - \mathbf{V}_{0,0}^{i+1}\| \\
&= \|\tfrac{1}{8}(2\mathbf{V}_{0,1}^{i} - \mathbf{V}_{0,2}^{i} - \mathbf{V}_{0,0}^{i}) + \tfrac{1}{8}(2\mathbf{V}_{1,1}^{i} - \mathbf{V}_{1,2}^{i} - \mathbf{V}_{1,0}^{i})\| \\
&\le \tfrac{1}{8}M_{0,0}^i + \tfrac{1}{8}M_{0,0}^i = \tfrac{1}{4}M_{0,0}^i.
\end{aligned} \tag{35}$$

Case 2 ($E-F-E$): consider $2\mathbf{V}_{0,2}^{i+1} - \mathbf{V}_{0,3}^{i+1} - \mathbf{V}_{0,1}^{i+1}$.

$$\begin{aligned}
&\|2\mathbf{V}_{0,2}^{i+1} - \mathbf{V}_{0,3}^{i+1} - \mathbf{V}_{0,1}^{i+1}\| \\
&= \|\tfrac{1}{16}(2\mathbf{V}_{0,2}^{i} - \mathbf{V}_{0,3}^{i} - \mathbf{V}_{0,1}^{i} + 2\mathbf{V}_{0,1}^{i} - \mathbf{V}_{0,2}^{i} - \mathbf{V}_{0,0}^{i} \\
&\quad + 2\mathbf{V}_{1,2}^{i} - \mathbf{V}_{1,3}^{i} - \mathbf{V}_{1,1}^{i} + 2\mathbf{V}_{1,1}^{i} - \mathbf{V}_{1,2}^{i} - \mathbf{V}_{1,0}^{i})\| \\
&\le \tfrac{1}{16}M_{0,0}^i + \tfrac{1}{16}M_{0,0}^i + \tfrac{1}{16}M_{0,0}^i + \tfrac{1}{16}M_{0,0}^i = \tfrac{1}{4}M_{0,0}^i.
\end{aligned} \tag{36}$$

Case 3 ($E-V-E$): consider $2\mathbf{V}_{1,1}^{i+1} - \mathbf{V}_{1,2}^{i+1} - \mathbf{V}_{1,0}^{i+1}$.

$$\begin{aligned}
&\|2\mathbf{V}_{1,1}^{i+1} - \mathbf{V}_{1,2}^{i+1} - \mathbf{V}_{1,0}^{i+1}\| \\
&= \|\tfrac{1}{32}(2\mathbf{V}_{0,1}^{i} - \mathbf{V}_{0,2}^{i} - \mathbf{V}_{0,0}^{i}) + \tfrac{3}{16}(2\mathbf{V}_{1,1}^{i} - \mathbf{V}_{1,2}^{i} - \mathbf{V}_{1,0}^{i}) \\
&\quad + \tfrac{1}{32}(2\mathbf{V}_{2,1}^{i} - \mathbf{V}_{2,2}^{i} - \mathbf{V}_{2,0}^{i})\| \\
&\le \tfrac{1}{32}M_{0,0}^i + \tfrac{3}{16}M_{0,0}^i + \tfrac{1}{32}M_{0,0}^i = \tfrac{1}{4}M_{0,0}^i.
\end{aligned} \tag{37}$$

Case 4 ($V-E-V$): consider $2\mathbf{V}_{1,2}^{i+1} - \mathbf{V}_{1,3}^{i+1} - \mathbf{V}_{1,1}^{i+1}$.

$$\begin{aligned}
&\|2\mathbf{V}_{1,2}^{i+1} - \mathbf{V}_{1,3}^{i+1} - \mathbf{V}_{1,1}^{i+1}\| \\
&= \|\tfrac{1}{64}(2\mathbf{V}_{0,2}^{i} - \mathbf{V}_{0,3}^{i} - \mathbf{V}_{0,1}^{i} + 2\mathbf{V}_{0,1}^{i} - \mathbf{V}_{0,2}^{i} - \mathbf{V}_{0,0}^{i}) \\
&\quad + \tfrac{3}{32}(2\mathbf{V}_{1,2}^{i} - \mathbf{V}_{1,3}^{i} - \mathbf{V}_{1,1}^{i} + 2\mathbf{V}_{1,1}^{i} - \mathbf{V}_{1,2}^{i} - \mathbf{V}_{1,0}^{i}) \\
&\quad + \tfrac{1}{64}(2\mathbf{V}_{2,2}^{i} - \mathbf{V}_{2,3}^{i} - \mathbf{V}_{2,1}^{i} + 2\mathbf{V}_{2,1}^{i} - \mathbf{V}_{2,2}^{i} - \mathbf{V}_{2,0}^{i})\| \\
&\le (\tfrac{1}{64} + \tfrac{1}{64} + \tfrac{3}{32} + \tfrac{3}{32} + \tfrac{1}{64} + \tfrac{1}{64})M_{0,0}^i = \tfrac{1}{4}M_{0,0}^i.
\end{aligned} \tag{38}$$

This completes the proof of the lemma. □

7 Appendix B: Convergence of $\mathbf{V}_{2N+2}^n$, ..., $\mathbf{V}_{2N+8}^n$

Note that if one can prove that

$$\lim_{n\to\infty} (T)^n = \lim_{n\to\infty} \begin{pmatrix} \bar{T} & \mathbf{0} \\ \bar{T}_{1,1} & \bar{T}_{1,2} \end{pmatrix}^n = T^* \equiv \begin{pmatrix} \bar{T}^* & \mathbf{0} \\ \bar{T}_{1,1}^* & \mathbf{0} \end{pmatrix} \tag{39}$$

where $\bar{T}^*$ is defined in (14) and $\bar{T}_{1,1}^*$ is a $7 \times (2N+1)$ version of $\bar{T}^*$, i.e.,

$$\bar{T}_{1,1}^* = \begin{pmatrix} \Delta_1 & \Delta_2 & \cdots & \Delta_{2N+1} \\ \Delta_1 & \Delta_2 & \cdots & \Delta_{2N+1} \\ \vdots & \vdots & \ddots & \vdots \\ \Delta_1 & \Delta_2 & \cdots & \Delta_{2N+1} \end{pmatrix}_{7\times(2N+1)}, \tag{40}$$

then, by (8), we have

$$\mathbf{V}_j^n \to \mathbf{V}_1^* \equiv \Delta_1 \mathbf{V}_1 + \Delta_2 \mathbf{V}_2 + \cdots + \Delta_{2N+1}\mathbf{V}_{2N+1}$$

for $j = 2N+2, 2N+3, ..., 2N+8$. Hence, to prove that $\mathbf{V}_{2N+2}^n$, ..., $\mathbf{V}_{2N+8}^n$ converge to $\mathbf{V}_1^*$, it is sufficient to show that (39) is true or, equivalently, to show that (i) $(\bar{T}_{1,2})^n$ converges to a 7×7 zero matrix when n tends to infinity, and (ii) the lower-left $7 \times (2N+1)$ block of $(T)^{2n}$ converges to $\bar{T}_{1,1}^*$. (i) is obvious because $\bar{T}_{1,2}$ contains non-negative entries and the sum of each row is smaller than one. To prove (ii), note that the sum of each row of $(T)^n$ is one and, from (i),

$$(\bar{T}_{1,2})^n \to \mathbf{0}.$$

Therefore, for each of the last 7 rows of $(T)^n$, the sum of the first $2N+1$ entries is close to one when n is large. On the other hand, when n is large, (14) is true, i.e., each column of $(\bar{T})^n$ has almost identical entries. Hence, computing an entry of the lower-left $7 \times (2N+1)$ block of $(T)^{2n} = (T)^n(T)^n$ is like multiplying $2N+1$ almost identical entries (in the same column of the upper-left $(2N+1)\times(2N+1)$ block of the second $(T)^n$) by $2N+1$ non-negative numbers whose sum is close to one (in the same row of the lower-left $7 \times (2N+1)$ block of the first $(T)^n$). Consequently the value of that entry in the lower-left $7 \times (2N+1)$ block of $(T)^{2n} = (T)^n(T)^n$ is close to the first $2N+1$ almost identical entries in the same column of the second $(T)^n$ and this completes the proof of (ii). □

8 Appendix C: Rate of Convergence of Φ_j^k

In this appendix we prove Lemma 5 of Section 2.2.1. Since Φ_1^k is symmetric to Φ_3^k, we only need to consider G_0^k, G_2^k and G_3^k for the lemma.

(i) G_0^k: For an edge point such as $\mathbf{V}_4^{i+1}$, we have

$$\begin{array}{l}\|\mathbf{V}_1^{i+1}-\mathbf{V}_4^{i+1}\| \\ = \|\sum_{j=4}^N \frac{3}{2N^2}(\mathbf{V}_{2j}^i-\mathbf{V}_1^i)+\sum_{j=3}^N \frac{1}{4N^2}(\mathbf{V}_{2j+1}^i-\mathbf{V}_1^i) \\ \quad +(\frac{3}{2N^2}-\frac{1}{16})(\mathbf{V}_2^i-\mathbf{V}_1^i)+(\frac{1}{4N^2}-\frac{1}{16})(\mathbf{V}_3^i-\mathbf{V}_1^i) \\ \quad +(\frac{3}{2N^2}-\frac{3}{8})(\mathbf{V}_4^i-\mathbf{V}_1^i)+(\frac{1}{4N^2}-\frac{1}{16})(\mathbf{V}_5^i-\mathbf{V}_1^i) \\ \quad +(\frac{3}{2N^2}-\frac{1}{16})(\mathbf{V}_6^i-\mathbf{V}_1^i)\| \\ \le \Big[\sum_{j=4}^N \frac{3}{2N^2}+\sum_{j=3}^N \frac{1}{4N^2}+|2(\frac{3}{2N^2}-\frac{1}{16})| \\ \quad +(\frac{3}{8}-\frac{3}{2N^2})+2(\frac{1}{16}-\frac{1}{4N^2})\Big]\,G_0^i \\ = \begin{cases} (\frac{3}{8}+\frac{7}{4N}-\frac{4}{N^2})G_0^i, & \text{if } N=3 \\ (\frac{5}{8}+\frac{7}{4N}-\frac{10}{N^2})G_0^i, & \text{if } N\ge 5 \end{cases}\end{array} \tag{41}$$

where G_0^i is defined in (19).

For a face point such as $\mathbf{V}_3^{i+1}$, we have

$$\begin{array}{l}\|\mathbf{V}_1^{i+1}-\mathbf{V}_3^{i+1}\| \\ = \|\sum_{j=3}^N \frac{3}{2N^2}(\mathbf{V}_{2j}^i-\mathbf{V}_1^i)+\sum_{j=2}^N \frac{1}{4N^2}(\mathbf{V}_{2j+1}^i-\mathbf{V}_1^i) \\ \quad +(\frac{3}{2N^2}-\frac{1}{4})(\mathbf{V}_2^i-\mathbf{V}_1^i)+(\frac{1}{4N^2}-\frac{1}{4})(\mathbf{V}_3^i-\mathbf{V}_1^i) \\ \quad +(\frac{3}{2N^2}-\frac{1}{4})(\mathbf{V}_4^i-\mathbf{V}_1^i) \\ \le \Big[\sum_{j=3}^N \frac{3}{2N^2}+\sum_{j=2}^N \frac{1}{4N^2}+2(\frac{1}{4}-\frac{3}{2N^2})+\frac{1}{4}-\frac{1}{4N^2}\Big]\,G_0^i \\ = (\frac{3}{4}+\frac{7}{4N}-\frac{13}{2N^2})G_0^i, \qquad N=3 \text{ or } N\ge 5.\end{array} \tag{42}$$

The other cases are similar to (41) or (42). Hence, we have the following inequality for $N=3$ or $N\ge 5$:

$$\begin{array}{rcl} G_0^{i+1} & \le & (\frac{3}{4}+\frac{7}{4N}-\frac{13}{2N^2})G_0^i \\ & \le & \left(\frac{3}{4}+\frac{7}{4N}-\frac{13}{2N^2}\right)^{i+1} G_0^0. \end{array} \tag{43}$$

(ii) G_3^k: For an edge point such as $\mathbf{V}_{2N+8}^{i+1}$, we have

$$\begin{array}{l}\|\mathbf{V}_4^{i+1}-\mathbf{V}_{2N+8}^{i+1}\| \\ = \|\frac{1}{16}(\mathbf{V}_{2N+8}^i+\mathbf{V}_{2N+7}^i-\mathbf{V}_6^i-\mathbf{V}_5^i)+\frac{5}{16}(\mathbf{V}_3^i-\mathbf{V}_1^i)\| \\ \le \|\frac{1}{16}(\mathbf{V}_{2N+8}^i-\mathbf{V}_4^i)+\frac{1}{16}(\mathbf{V}_{2N+7}^i-\mathbf{V}_4^i) \\ \quad +\frac{1}{16}(\mathbf{V}_4^i-\mathbf{V}_6^i)+\frac{1}{16}(\mathbf{V}_4^i-\mathbf{V}_5^i)+\frac{5}{16}(\mathbf{V}_3^i-\mathbf{V}_1^i)\| \\ \le \frac{9}{16}\max\{G_0^i,G_3^i\}\end{array} \tag{44}$$

where G_0^i and G_3^i are defined in (19).
For a face point such as $\mathbf{V}_3^{i+1}$, we have

$$\begin{array}{l}\|\mathbf{V}_4^{i+1}-\mathbf{V}_3^{i+1}\| \\ = \|\frac{3}{16}(\mathbf{V}_2^i+\mathbf{V}_3^i)-\frac{1}{16}(\mathbf{V}_6^i+\mathbf{V}_5^i)-\frac{1}{8}(\mathbf{V}_1^i+\mathbf{V}_4^i)\| \\ \le \|\frac{3}{16}(\mathbf{V}_2^i-\mathbf{V}_1^i)+\frac{3}{16}(\mathbf{V}_3^i-\mathbf{V}_4^i)+\frac{1}{16}(\mathbf{V}_1^i-\mathbf{V}_6^i) \\ \quad +\frac{1}{16}(\mathbf{V}_4^i-\mathbf{V}_5^i)\| \\ \le \frac{1}{2}\max\{G_0^i,G_3^i\}.\end{array} \tag{45}$$

For a vertex point such as $\mathbf{V}_{2n+7}^{i+1}$, we have

$$\begin{array}{l}\|\mathbf{V}_4^{i+1}-\mathbf{V}_{2N+7}^{i+1}\| \\ = \|\frac{3}{16}\mathbf{V}_4^i-\frac{9}{32}\mathbf{V}_1^i+\frac{1}{32}(\mathbf{V}_3^i+\mathbf{V}_5^i)+\frac{3}{32}\mathbf{V}_{2N+7}^i \\ \quad -\frac{3}{64}(\mathbf{V}_6^i+\mathbf{V}_2^i)+\frac{1}{64}(\mathbf{V}_{2N+8}^i+\mathbf{V}_{2N+6}^i)\| \\ \le \|\frac{1}{64}(\mathbf{V}_{2N+8}^i-\mathbf{V}_4^i)+\frac{3}{32}(\mathbf{V}_{2N+7}^i-\mathbf{V}_4^i) \\ \quad +\frac{1}{64}(\mathbf{V}_{2N+6}^i-\mathbf{V}_4^i)+\frac{9}{32}(\mathbf{V}_4^i-\mathbf{V}_1^i)+\frac{3}{64}(\mathbf{V}_1^i-\mathbf{V}_6^i) \\ \quad +\frac{3}{64}(\mathbf{V}_1^i-\mathbf{V}_2^i)+\frac{1}{32}(\mathbf{V}_3^i-\mathbf{V}_1^i)+\frac{1}{32}(\mathbf{V}_5^i-\mathbf{V}_1^i) \\ \le \frac{9}{16}\max\{G_0^i,G_3^i\}.\end{array} \tag{46}$$

The other cases are similar to these cases. Hence, by combining the results of (44), (45) and (46), we have

$$\begin{array}{rcl} G_3^{i+1} & \le & \frac{9}{16}\max\{G_0^i,G_3^i\} \\ & \le & \frac{9}{16}(\frac{3}{4}+\frac{7}{4N}-\frac{13}{2N^2})^i\max\{G_0^0,G_3^0\}. \end{array} \tag{47}$$

The second inequality of (47) follows from (43). (47) works for $N=3$ or $N\ge 5$.

(iii) G_2^k: For an edge point such as $\mathbf{V}_{2N+6}^{i+1}$, we have

$$\begin{array}{l}\|\mathbf{V}_{2N+6}^{i+1}-\mathbf{V}_5^{i+1}\| \\ = \|-\frac{3}{16}(\mathbf{V}_1^i+\mathbf{V}_6^i)+\frac{1}{8}(\mathbf{V}_4^i+\mathbf{V}_5^i) \\ \quad +\frac{1}{16}(\mathbf{V}_{2N+7}^i+\mathbf{V}_{2N+6}^i)\| \\ = \|\frac{3}{16}(\mathbf{V}_4^i-\mathbf{V}_1^i)+\frac{3}{16}(\mathbf{V}_5^i-\mathbf{V}_6^i)+\frac{1}{16}(\mathbf{V}_{2N+7}^i-\mathbf{V}_4^i) \\ \quad +\frac{1}{16}(\mathbf{V}_{2N+6}^i-\mathbf{V}_5^i)\| \\ \le \frac{1}{2}\max\{G_1^i,G_2^i,G_3^i\}.\end{array} \tag{48}$$

For a vertex point such as $\mathbf{V}_{2N+2}^{i+1}$, we have

$$\begin{array}{l}\|\mathbf{V}_{2N+2}^{i+1}-\mathbf{V}_5^{i+1}\| \\ = \|\frac{3}{32}(\mathbf{V}_{2N+6}^i-\mathbf{V}_5^i)-\frac{1}{64}(\mathbf{V}_{2N+2}^i-\mathbf{V}_5^i) \\ \quad -\frac{3}{32}(\mathbf{V}_{2N+3}^i+\mathbf{V}_5^i)+\frac{1}{64}(\mathbf{V}_{2N+4}^i-\mathbf{V}_6^i) \\ \quad +\frac{1}{64}(\mathbf{V}_{2N+7}^i-\mathbf{V}_4^i)+\frac{9}{64}(\mathbf{V}_5^i-\mathbf{V}_6^i) \\ \quad +\frac{9}{64}(\mathbf{V}_5^i-\mathbf{V}_4^i)+\frac{15}{64}(\mathbf{V}_5^i-\mathbf{V}_1^i)\| \\ \le \frac{3}{4}\max\{G_1^i,G_2^i,G_3^i\}.\end{array} \tag{49}$$

The other cases are similar to these two cases. Hence, by combining the results of (48), (49), (43) and (47), we have

$$\begin{array}{rcl} G_2^{i+1} & \le & \frac{3}{4}\max\{G_1^i,G_2^i,G_3^i\} \\ & \le & \begin{cases} (\frac{3}{4})^{i+1}G^0, & \text{if } N=3 \\ (\frac{3}{4})(\frac{3N^2+7N-26}{4N^2})^i G^0, & \text{if } N\ge 5 \end{cases} \end{array} \tag{50}$$

where $G^0=\max\{G_0^0,G_1^0,G_2^0,G_3^0\}$. The lemma now follows from (43), (47) and (50). □

9 Appendix D: Proof of (26)

The proof of Lemma 3 shows that the norms of most of the second order forward differences of the control points of Π_3^k satisfy the inequality

$$\|2\mathbf{A}-\mathbf{B}-\mathbf{C}\| \le \frac{1}{4}Z_0^{k-1}$$

except $2\mathbf{V}_1^k-\mathbf{V}_2^k-\mathbf{V}_6^k$, $2\mathbf{V}_6^k-\mathbf{V}_1^k-\mathbf{V}_{2N+4}^k$ and $2\mathbf{V}_4^k-\mathbf{V}_1^k-\mathbf{V}_{2N+7}^k$. The last two cases are similar. Hence, we only need to consider the first two cases.

In the second case we have

$$\begin{array}{l}\|2\mathbf{V}_6^{i+1}-\mathbf{V}_1^{i+1}-\mathbf{V}_{2N+4}^{i+1}\| \\ \quad = \quad \|\frac{1}{64N^2}\{N^2(2\mathbf{V}_7^i-\mathbf{V}_8^i-\mathbf{V}_{2N+5}^i)\end{array}$$

$$
\begin{aligned}
&+N^2(2\mathbf{V}_5^i - \mathbf{V}_{2N+3}^i - \mathbf{V}_4^i)\\
&+6N^2(2\mathbf{V}_6^i - \mathbf{V}_1^i - \mathbf{V}_{2N+4}^i)\\
&+8\sum_{j=1}^{N}(2\mathbf{V}_{2[j\%N+1]}^i - \mathbf{V}_{2j+1}^i - \mathbf{V}_{2[j\%N+1]+1}^i)\\
&+(8N^2-56)(-2\mathbf{V}_1^i + \mathbf{V}_4^i + \mathbf{V}_8^i)\\
&+56\sum_{j=3}^{N+1}(2\mathbf{V}_1^i - \mathbf{V}_{2[(j-1)\%N+1]}^i - \mathbf{V}_{2[(j+1)\%N+1]}^i)\}\|\\
\leq\ & (\frac{1}{4}+\frac{1}{N}-\frac{7}{4N^2})Z_0^i, \qquad N=3 \text{ or } N\geq 5
\end{aligned}
$$

where Z_0^i is the second order norm of $\mathbf{S}_0^i$. In the above derivation, $\mathbf{V}_8^i$ should be replaced with $\mathbf{V}_2^i$ when $N=3$.

In the first case, when $N \geq 5$, we have

$$
\begin{aligned}
&\|2\mathbf{V}_1^{i+1} - \mathbf{V}_2^{i+1} - \mathbf{V}_6^{i+1}\|\\
=\ & \frac{1}{16N^2}\|\sum_{j=1}^{N}4(\mathbf{V}_{2j-1}^i - 2\mathbf{V}_{2j}^i + \mathbf{V}_{2j+1}^i)\\
&+N^2(2\mathbf{V}_2^i - \mathbf{V}_{2N+1}^i - \mathbf{V}_3^i)\\
&+N^2(2\mathbf{V}_6^i - \mathbf{V}_7^i - \mathbf{V}_5^i)\\
&+(N^2-28)(2\mathbf{V}_1^i - \mathbf{V}_4^i - \mathbf{V}_{2N}^i)\\
&+(N^2-28)(2\mathbf{V}_1^i - \mathbf{V}_4^i - \mathbf{V}_8^i)\\
&-\sum_{j=5}^{N-1}28(2\mathbf{V}_1^i - \mathbf{V}_{2j}^i - \mathbf{V}_{2(j-2)}^i)\\
&-28(2\mathbf{V}_1^i - \mathbf{V}_{2N-4}^i - \mathbf{V}_{2N}^i)\\
&-28(2\mathbf{V}_1^i - \mathbf{V}_{2N-2}^i - \mathbf{V}_2^i)\\
&+(8N^2-28)(2\mathbf{V}_1^i - \mathbf{V}_2^i - \mathbf{V}_6^i)\|\\
\leq\ & \begin{cases} (\frac{1}{2}+\frac{1}{4N}+\frac{21}{4N^2})Z_0^i, & \text{if } N=5\\ (\frac{3}{4}+\frac{2}{4N}-\frac{21}{2N^2})Z_0^i, & \text{if } N>5 \end{cases}.
\end{aligned}
$$

In the first summation, one should use $\mathbf{V}_{2N+1}^i$ for $\mathbf{V}_{2j-1}^i$ when $j=1$. The difference between the case $N=5$ and $N\geq 6$ comes from the fact that (N^2-28) is negative when $N=5$. when $N=3$, we have

$$
\begin{aligned}
&\|2\mathbf{V}_1^{i+1} - \mathbf{V}_2^{i+1} - \mathbf{V}_6^{i+1}\|\\
=\ & \frac{1}{144}\|5(2\mathbf{V}_2^i - \mathbf{V}_3^i - \mathbf{V}_7^i) + 5(2\mathbf{V}_6^i - \mathbf{V}_7^i - \mathbf{V}_5^i)\\
&-4(2\mathbf{V}_4^i - \mathbf{V}_3^i - \mathbf{V}_5^i) - 19(2\mathbf{V}_1^i - \mathbf{V}_4^i - \mathbf{V}_2^i)\\
&-19(2\mathbf{V}_1^i - \mathbf{V}_4^i - \mathbf{V}_6^i) + 44(2\mathbf{V}_1^i - \mathbf{V}_2^i - \mathbf{V}_6^i)\|\\
\leq\ & \frac{2}{3}Z_0^i, \qquad \text{when } N=3
\end{aligned}
$$

Consequently, from the above results we have the first part of (26). The second part of (26) follows from the observation that the norms of second order forward differences similar to $2\mathbf{V}_1^{i+1} - \mathbf{V}_2^{i+1} - \mathbf{V}_6^{i+1}$ dominates the other second order forward differences in all subsequent norm computation. □

References

[1] Austin S, Jerard R, Drysdale R, 1997. Comparison of discretization algorithms for NURBS surfaces with application to numerically controlled machining, *Computer Aided Design 29* 1, 71-83.

[2] Biermann, H., Kristjansson, D., and Zorin, D. 2001. Approximate Boolean Operations on Free-Form Solids. In *Proceedings of SIGGRAPH 2001*, 185-194.

[3] Catmull E, and Clark J, 1978. Recursively Generated B-spline Surfaces on Arbitrary Topological Meshes. *Computer-Aided Design 10*, 6, 350-355.

[4] Cheng F, 1992. Estimating Subdivision Depths for Rational Curves and Surfaces. *ACM Trans. on Graphics 11*, 2 140-151.

[5] Doo D, and Sabin M, 1978. Behavior of Recursive Division Surfaces near Extraordinary Points. *Computer-Aided Design 10*, 6, 356-360.

[6] Halstead M, Kass M, DeRose T, 1993. Efficient, Fair Interpolation Using Catmull-Clark Surfaces. In *Proceedings of SIGGRAPH 1993*, 35-44.

[7] Litke N, Levin A, and Schröder P, 2001. Trimming for Subdivision Surfaces. *Computer Aided Geometric Design 18*, 5, 463-481.

[8] Lutterkort D, and Peters J, 2001, Tight linear envelopes for splines. *Numerische Mathematik 89*, 4, 735-748.

[9] Sheldon M Ross, *Introduction to Probability Models*. Academic Press, Inc., Orlando, Florida, 1985.

[10] Sederberg T W, 1998. Non-Uniform Recursive Subdivision Surfaces. In *Proceedings of SIGGRAPH 1999*, 387-394.

[11] Stam J, 1998. Exact Evaluation of Catmull-Clark Subdivision Surfaces at Arbitrary Parameter Values. In *Proceedings of SIGGRAPH 1998*, 395-404.

[12] Wang H, Qin K, 2004. Estimating Subidivision Depth of Catmull-Clark Surfaces. *J. Comput. Sci. & Technol. 19*, 5, 657-664.

[13] Zorin D, Schröder P, and Sweldens W, Interactive Multiresolution Mesh Editing. In *Proceedings of SIGGRAPH 1997*, 259-268.